ELSEVIER

Nuclear Instruments and Methods in Physics Research A 443 (2000) 451–463

NUCLEAR INSTRUMENTS & METHODS IN PHYSICS RESEARCH Section A

www.elsevier.nl/locate/nima

# An electronic clock for correlated noise corrections

W.J. Llope*, N. Adams, K.K. Kainz

*T.W. Bonner Nuclear Laboratory, Rice University, MS 315, 6100 S. Main Street, Houston, TX 77005-1892, USA*

Received 26 August 1999; accepted 22 October 1999

**Abstract**

An inexpensive and portable approach is presented to measure the time of occurrence of an experimental event as measured by a specific electronic clock. The clock resets in active synchronization with the experimental AC-power cycle. This allows an efficient and complete correction for correlated noise contributions to pulse area and time measurements of detector channels equipped with PhotoMultiplier Tubes. The electronic board that was developed will be described. The performance for the treatment of correlated noise in experimental data taken at the BNL-AGS facility, and analyses of spectral decompositions of this noise, will also be described. 

*PACS:* 84.30.Ng; 7.50.-e; 89.20. + a

*Keywords:* Noise; Correlated; Common mode; AC line; Ground loop; ADC pedestal; 60 Hz; Synchronized electronic clock

## 1. Introduction

Despite dedicated efforts to insure otherwise, a voltage ripple with the same frequency as the main AC power line (60 Hz in the US) but a complicated shape and amplitude may exist on the electrical ground used in an experiment. The cause of the ripple is the existence somewhere in the experiment of at least one electrical path between the experimental ground and other grounds. These "dirty" grounds may be at different mean voltages relative to the experimental ground and may be correlated with the AC power with different phases, line shapes and amplitudes. Generally, experimenters use oscilloscopes and voltmeters to locate unwanted electrical connection(s) in the experiment that tie the experimental ground to dirty grounds. The most egregious paths can generally be located and removed in this manner, and the grounds may hence appear very clean when only the experiment itself is fully powered up. During an actual run, however, the experimental ground may be compromised in ways beyond the control of the experimenters. The contaminating voltage ripple is a noise current which may differ for different detectors in the experiment and for different elements of any given detector, and may be weakly time dependent over periods of hours. The digitization in an Analog-Digital Converter (ADC) of the total charge of electrical pulses from active detector elements is then made versus a baseline ground that itself carries current. This smears ADC data, possibly significantly, and makes less significant all quantities inferred from it. The custom circuit developed to

* Corresponding author.

0168-9002/00/$ - see front matter 
PII: S0168-9002(99)01164-X

address this problem for Experiment 896 [1] at the BNL-AGS, and its performance for correlated noise corrections, is described here.

Detector channels involving PhotoMultiplier Tubes (PMTs) are particularly sensitive to such ground contaminations, as PMTs are nearly perfect amplifiers. Depending on certain factors such as the widths of ADC gates that are used, even a few millivolts of correlated noise can significantly worsen the ADC resolution both on the pedestal and for hits. The Time of Flight (TOF) system in BNL-AGS Experiment 896 is composed of $\sim 190$ Bicron BC404 plastic scintillator slats of various dimensions each read out by two PMTs (Hamamatsu R2076 or 1398 depending on the slat). The signals from the E896 TOF System have a width of $\sim 10$ ns FWHM and peak at about $-300$ mV for single hits of relativistic charge $Z = 1$ particles. This implies that the integrated charge in a typical PMT pulse for a $Z = 1$ hit is in the order of 45 pC into 50 Ω. For this system, the ADC gate width used is 200 ns wide. If the ripple in the ground at the time of a particle hit is 2 mV, the integral within the same 200 ns wide gate is $\sim 8$ pC into 50 Ω, which is $\sim 10\%$ of the charge measured for hits and *time dependent*. Depending on how ADC information from a particular detector is used in subsequent analyses, correlated noise may thus have far reaching implications. The resolution on the charge $|Z|/e$ of particles striking (thin) E896 TOF slats, inferred from the TOF ADC values, can be worsened. Corrections to the TOF timing information based on the ADC information, i.e. "slewing" corrections, [2] would be degraded, worsening the TOF timing performance. There are other detectors in E896 that include the PMT read-out of scintillation or Cherenkov light. These detectors include the Multi-Functional Neutron Spectrometer (MUFFINS), the Beam Counters (BCs), the Exit Charge Detector (ECD), and the MuLTiplicity detector (MLT). Correlated noise degrades $|Z|/e$ measurements and the quality of the slewing corrections for the MUFFINs and BC data, and degrades inferences on the event centrality based on the MLT and ECD data.

This paper is organized as follows. Section 2 describes the apparent symptoms of a correlated noise problem, using as an example those in experimental data collected by the E896 Collaboration [1] during the Spring 1998 run of 11.5 GeV/c/N $^{197}$Au beams at the BNL-AGS. As alluded to above, the E896 experiment is composed of many different subsystems arranged in a mechanically and electrically complicated configuration. There are two large spectroscopic magnets in E896, and many more beam line magnets nearby. As will be shown, correlated noise is rampant in E896 during full beam-on running conditions, although the experimental grounds are clean otherwise. The general solution chosen to combat this problem offline involves custom electronics which are described in Section 3. Sections 4 and 5 describe the results obtained when this information was inserted into the E896 data stream during full beam-on running conditions. The summary and conclusions are presented in Section 6.

## 2. The symptom

In general, an ADC pedestal for the PMT-equipped detector channel has contributions from the intrinsic offsets of the ADC itself, and the PMTs dark current. For the Hamamatsu R2076 and 1398 PMTs and the LeCroy 1885F ADCs used in the E896 TOF System, these contributions typically result in a pedestal variance in the order of 3–5 ADC channels. A correlation between the pedestals of different detector channels is the unambiguous signature of correlated noise, also known as "common mode noise," or "ground loops."

All of the $\sim 600$ ADC pedestals in five different detector systems in E896 are, in some way, highly correlated during full running conditions. An example is shown in Fig. 1 for two PMTs attached to two different E896 TOF slats. The upper right and lower left frames in Fig. 1 indicate that the ADC pedestals for these two channels have variances on the order of 40 channels, which is an order of magnitude larger than that expected in the absence of correlated noise.

To recover the needed ADC resolution, one must measure the contribution to the ADC values arising solely from the correlated noise component in each experimental event. One method is to add one or more "blackened PMTs" (bPMTs) to the

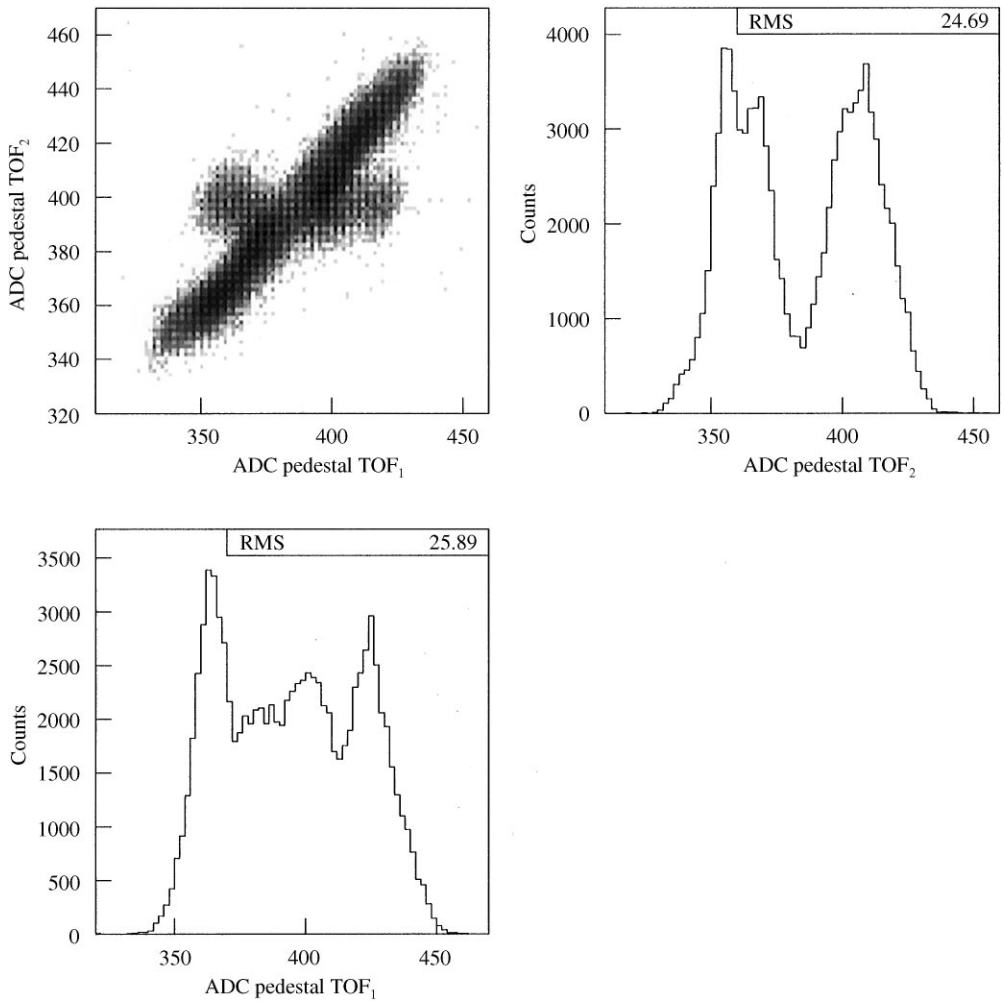


Fig. 1. Two typical ADC pedestal distributions for two channels in the E896-TOF System during the Au98 run (upper right and lower left), and their correlation in two dimensions (upper left). The axes out of the page are logarithmic.

detector, and digitizing these in ADCs exactly as if these bPMTs were attached to active elements. Such blackened PMTs are optically isolated by definition, but as they are mechanically and electrically part of the detector, the ADC values measured are, up to (time-independent) offsets, exactly the correlated noise contribution event by event.

If the correlation between the ADC pedestal from an active channel and that from a bPMT channel is sufficiently strong and single valued (i.e. something like the left frame in Fig. 2, the ADC values in active channels can be corrected with some efficiency for the correlated noise contribution using the value of the bPMT in each experimental event. One makes two passes through the experimental data. First one records the correlation between the ADC values for the active channel versus the ADC values from a bPMT, in only those events when the active channel is known to be not struck by a particle. Once this dependence versus one (or more) bPMTs is known for each active channel, in the second pass through the data the bPMT correction can be applied to the active

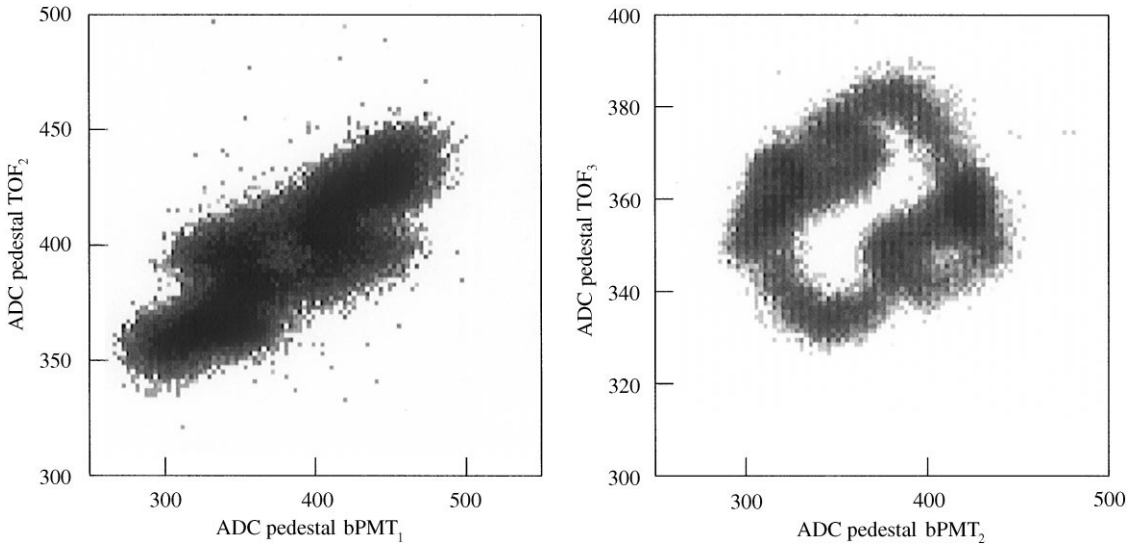


Fig. 2. Correlations of the ADC pedestals from two active channels (each ordinate) and two bPMT channels (each abscissa) in the TOF system in pedestal-only events. The axes out of the page are logarithmic.

channels in all events, independent of whether the active channel was struck by a particle or not.

However, there is a crucial shortcoming of such bPMT-based approaches. A complete offline correction is possible only if this correlation is indeed strong and single-valued. That is, the blackened PMT must sit on the same local ground as the PMT to be corrected. In electrically simple experiments, i.e. if there is only one or two variants of the (dirty) electrical ground seen by different detector elements, a handful of blackened PMTs could provide all of the information needed for a sufficient correction for correlated noise. In more complicated experiments, i.e. anything on a heavy-ion beam-line, it is possible that innumerable different local grounds exist with different shapes, amplitudes, and phases. An example of a detector channel that cannot efficiently be corrected using a particular bPMT is seen in the right frame of Fig. 2.

Shown in Fig. 3 is the correlation of ADC pedestals from a number of detectors in E896 versus a particular time recorded for each experimental event and inserted into the main data stream. This time is obtained from a clock, described below, that resets at 60 Hz in active synchronization with the experimental AC power. These plots can be considered oscilloscope traces for ADC pedestals where the horizontal axis is $16.\overline{6}$ ms in total, and the "trigger" is by definition always at exactly the same phase relative to the experimental AC power line. Clear signatures of correlated noise are in fact seen in *all* PMT-equipped channels in this experiment during full beam-on running conditions. It is also clear that there are many variants of the (dirty) grounds local to the different subdetectors in E896, and indeed differing local grounds also exist between different channels in a given subdetector.

If one wanted to combat the noise problem in E896 with blackened PMTs, one would need *many* of them, and the time and tenacity to find *all* of the different local grounds at work in the experiment. A more universal and technically simpler correction is possible given the availability of a single number for each experimental event. This number is the time the event occurred as measured within $16.\overline{6}$ ms intervals that are actively synchronized with the experimental AC power, i.e. the time defining the horizontal axis of Fig. 3. The custom electronics we developed that allows this number to be trivially inserted into any experimental data stream

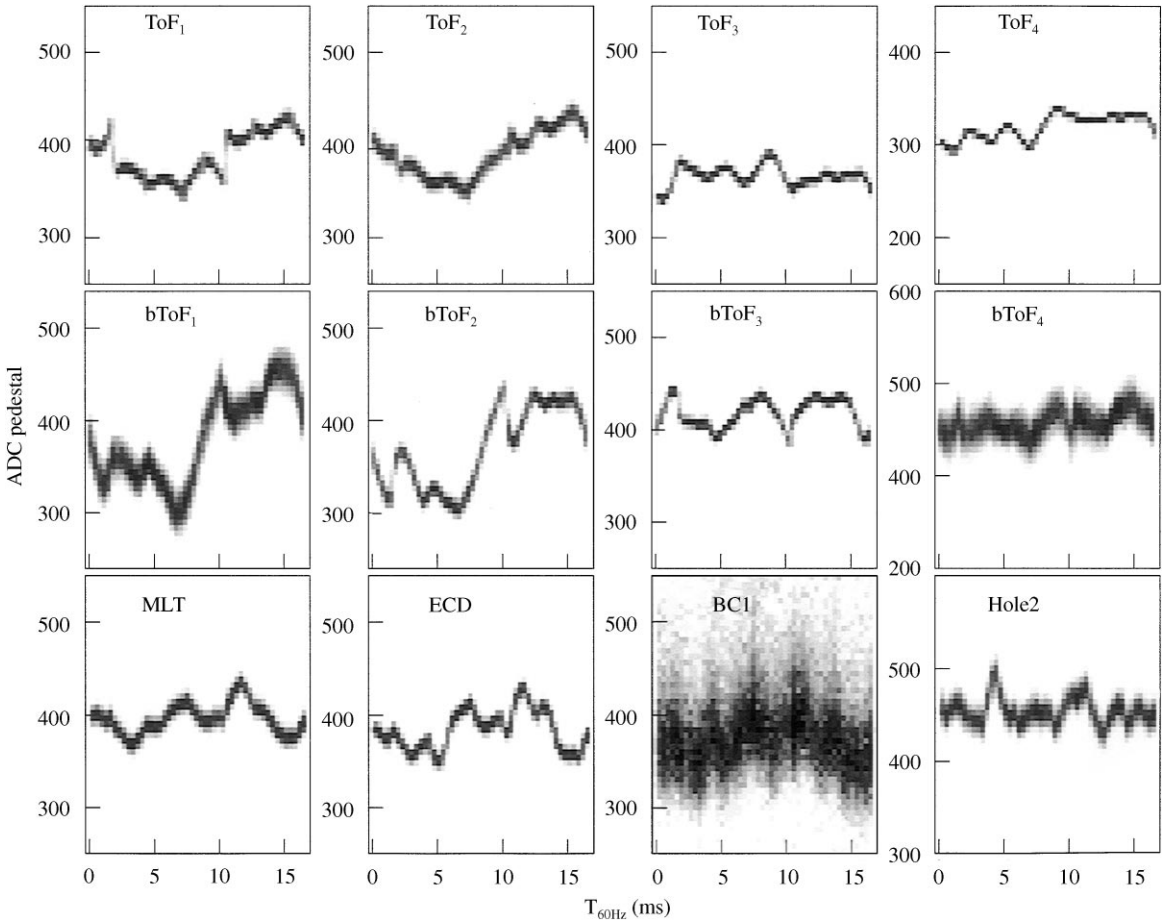


Fig. 3. The ADC pedestals from a sampling of PMT-equipped detectors in E896, as labelled in each frame, versus a particular event time described in the text. The axes out of the page are logarithmic.

for each experimental event is described in the next section.

## 3. The ramp

Given the time that each event occurs, measured relative to time intervals that are actively synchronized with the experimental AC power, one can correct completely for correlated noise offline. In experiments in the US, the line frequency is 60 Hz. One thus can use an AC line-synchronized 60 Hz pulser and a latching scaler to provide such clock information to a data acquisition system [3]. We describe here another approach. The present approach was developed primarily because it is more suitable for integration into the E896 data stream than the pulser + latching scaler approach, although the circuit we built is also smaller, considerably cheaper, and more generally portable. The present device can be made part of any experiment that has one spare AC power socket and one spare ADC channel.

The circuit generates a precision negative-voltage sawtooth waveform which resets from $V_{\max}$ to $V_{\min}$ in active synchronization with the experimental AC power line. The output is sent to a spare channel of the ADCs used to digitize the detector

signals. When an event occurs, the ADC channel connected to the ramp is thus gated at the same absolute time as the detector channel ADCs are gated. Experimental gates are typically 100–200 ns wide, which is a factor of $10^5$ shorter than the $16.\overline{6}$ ms period of the AC line. This implies the gating of the ADC channel connected to the ramp digitizes a very thin vertical slice, so the pulse area measured by the ramp ADC is thus effectively just a measurement of the instantaneous value of the ramp voltage at the time the experimental event occurs.

By construction, the ramp voltage so measured is related linearly to the time within the active AC line-synchronized $16.\overline{6}$ ms intervals. The depiction of an ADC pedestal, from detectors anywhere in the experiment, versus the (single) ramp ADC value in the same event thus measures exactly, event by event, the time dependence of the dirty experimental ground local to each detector channel. This allows straightforward and complete offline corrections (examples described below), no matter how many different local grounds exist in the experiment. As there is by definition a ramp value for every experimental event, the correction (described in the next section) is $\sim 100\%$ efficient in practice.

The circuit that was built in the early 1998 and used in the E896 1998 Au run is shown schematically in Fig. 4. The circuit is connected to the experimental AC power using a US-standard three

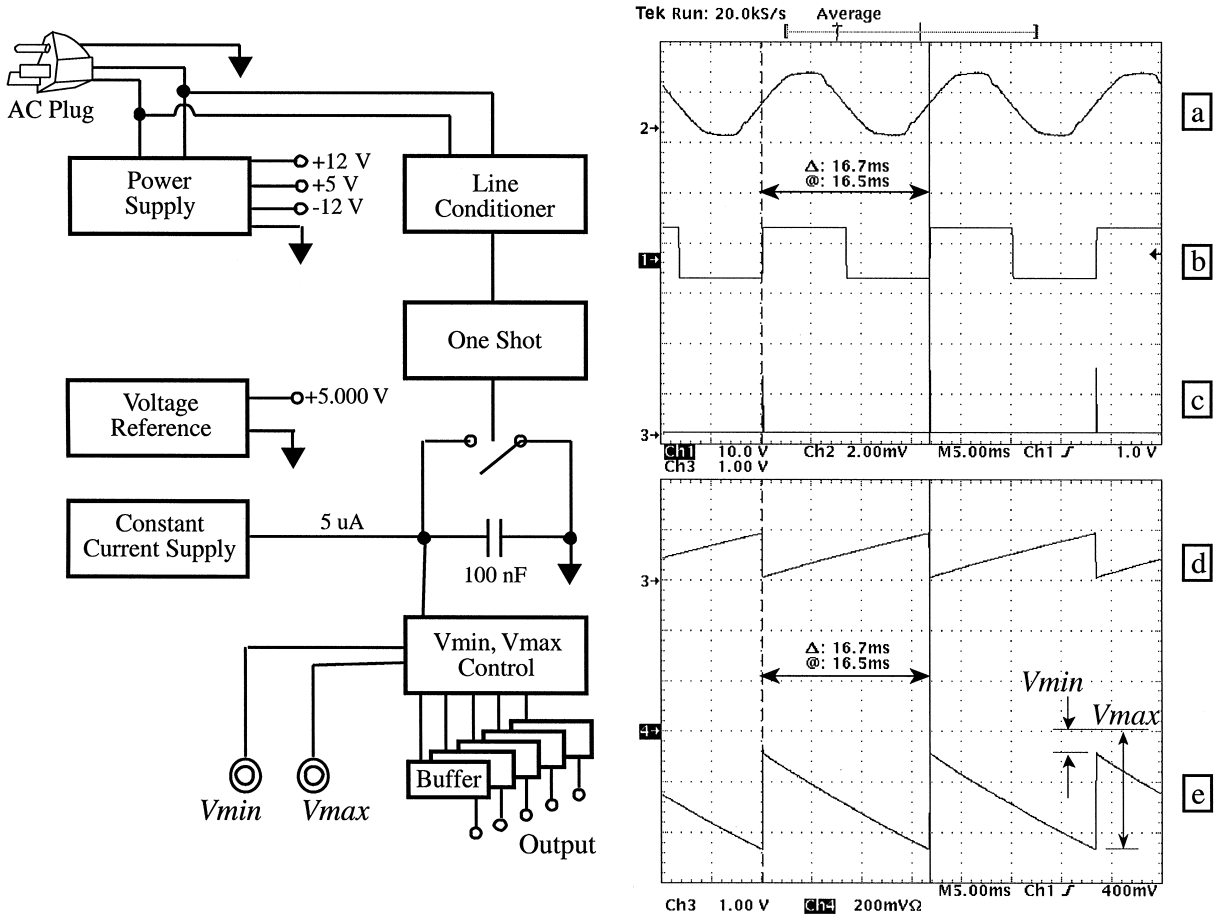


Fig. 4. On the left side, a schematic depiction of the present synchronized clock circuit, and on the right are oscilloscope traces for the signals at various stages of the signal processing.

prong plug. The AC voltage is shown, attenuated by 100 dB, as trace (a) in this figure. The neutral and phase lines from the AC plug are sent to a power supply, which provides the low voltages used by the circuit, and to a line conditioner. The line conditioner searches for the time at which the experimental AC power crosses zero volts from below, and generates a bipolar square wave in phase with this time, and hence with the AC power cycle, as seen in trace (b). The bipolar square wave is sent to a "one-shot," which controls a switch. The leading edges of the one-shot output, shown in trace (c), open the switch and falling edges close the switch.

A voltage reference and a constant current supply continuously add charge to a 100 nF capacitor (trace d), and by a related amount to the rest of the circuit. This produces the precision voltage ramp, shown in trace (e). When the next 60 Hz cycle begins, i.e. on a leading edge of trace (b), the one shot closes the switch and discharges the capacitor. When the circuit senses the capacitor is fully discharged, which approximately 3 μs later, the one-shot reopens the switch and the output (trace e) returns to $V_{\min}$. Current then begins flowing into the capacitor again, charging it and producing an output voltage that again becomes more negative in precise linearity with the time within the present AC cycle.

The synchronization is active, occurring independently for each cycle of the AC power. Thus, in principle there is nothing in the present circuit that makes it specific to 60 Hz line frequencies. The device should work without modification for others, such as are used in experiments abroad.

The discharging of the capacitor implies a "dead time" of the circuit of $\sim 3\ \mu s/16.\overline{6}$ ms, or about 0.02%. The current out of the constant current supply is generated against a 5.000 V voltage reference, which holds the voltage on the capacitor precise to one part in a few thousand. This implies that the circuit provides the time within the AC line-synchronized $16.\overline{6}$ ms periods with a resolution of a few microseconds. Such a time resolution is sufficient to correct for typical correlated noise levels – typically one needs sufficient statistical certainty in only 50–100 bins of the 60 Hz time in order to perform a complete correction (as shown below).

The value of $V_{\min}$ and $V_{\max}$ are adjustable via externally mounted potentiometers. This allows the device to be trivially implemented in other experiments, which may use ADC gates of different widths or ADC modules with different full scale ranges or charge conversion factors. The present circuit uses buffers to produce five copies of the ramp signal, each of which was sent to a spare channel in five different TOF ADC modules in the E896 TOF system. In the end only one output channel was actually needed, as the circuit proved to be very stable and its data easy to understand.

The circuit is packaged in a small metal box with external signal connectors and the pots for the $V_{\min}$ and $V_{\max}$ control, which is shown in Fig. 5. The cost was on the whole about $100.

## 4. The performance

The event-inclusive distribution of ADC values for the ADC channel connected to the present ramp circuit should, except for spill-structure or other known event trigger time correlations, be essentially flat. Such a distribution for one data-taking run from the E896 Au98 run is shown in Fig. 6. The raw ramp ADC distribution is shown in the solid histogram. The dashed histogram depicts the same ramp ADC distribution following the subtraction of the two intrinsic pedestals in the (dual range) LRS 1885F ADCs. This subtraction was done following a measurement of these two intrinsic pedestals for each ADC channel using calibration logic internal to the ADC and a Tcl/Tk script [4].

Based on the dashed histogram in Fig. 6, the times $t_0$ at which new 60 Hz cycles begin (and the ramp resets to the voltage $V_{\min}$) are identified as those events with a pedestal-subtracted ramp ADC value of 0. The time $16.\overline{6}$ ms later is identified as an pedestal-subtracted ramp ADC value of $\sim 15\,000$. Thus the event time, $T_{60\ \mathrm{Hz}}$, in milliseconds relative to the AC cycle is then computed from the intrinsic pedestal-subtracted ramp ADC values in each event, $\mathrm{ADC}_{\mathrm{ramp}}$, simply from $T_{60\ \mathrm{Hz}} = (16.67\ \mathrm{ms})^{*}\mathrm{ADC}_{\mathrm{ramp}}/15\,000$. This is how the

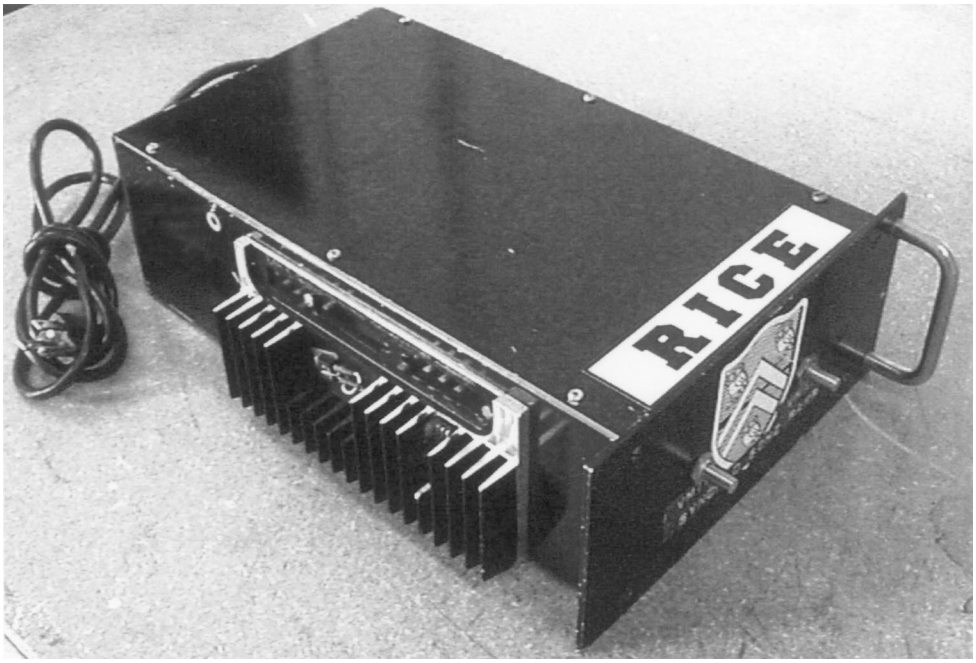


Fig. 5. A side and front view of ramp generator box. Visible on the front panel are the two dials for the $V_{min}$ and $V_{max}$ control, and on the side are cooling vanes. Not visible on the back of the box are the five BNC connectors for the output of the ramp signals.

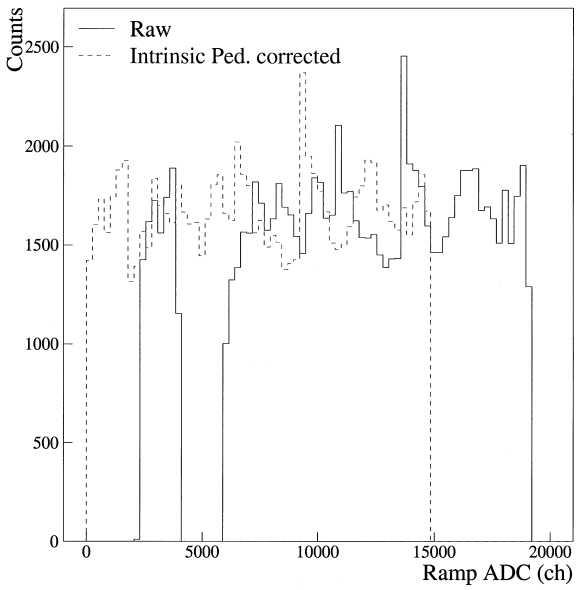


Fig. 6. An example from one run of the event-inclusive distribution of ADC values for the channel connected to the present ramp circuit. The raw ramp ADC distribution is shown in the solid line, while the dotted line shows the ramp ADC distribution following the subtraction of the two intrinsic pedestals per channel in the (dual-range) LRS 1885F ADCs.

horizontal axis of Figs. 3 and 7 was obtained. It should be noted that, as the digitization of the ramp voltage is performed entirely in the counting house, and no PMTs are involved, there is no correlated noise contribution in the ramp ADC values themselves. This allows the ramp ADC values to be applied directly for the noise correction of all of the PMT-equipped detector channels in the experiment.

During the 1998 Au run, hundreds of data runs were recorded to tape in E896, and each was approximately 20 min long ($\sim$200 k events/data run). This is well matched to the time scale of roughly hours over which the correlated noise line shapes for a given detector channel slowly drift. Thus, the recording of the pedestal profiles for each of the $\sim$600 ADC pedestals in E896 once per data run allows sufficiently accurate corrections.

A correction based on the present device involves two passes through the experimental data. In the first, the correlated noise "profiles" versus the ramp ADC are collected and saved for each PMT in the experiment. Shown in Fig. 7 are such profiles, i.e. the ordinates are average values of an ADC

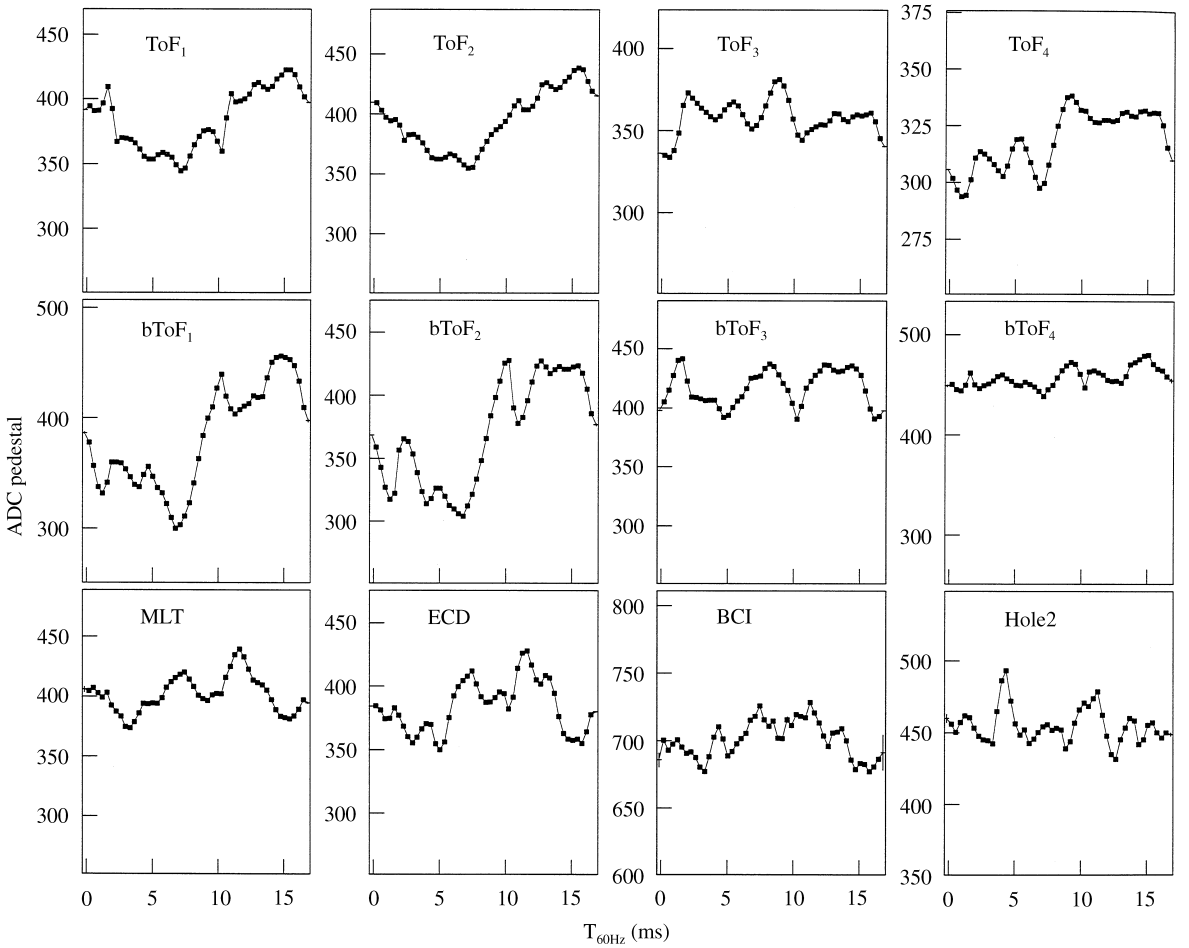


Fig. 7. Profile histograms of the correlation of the average ADC pedestals in a single experimental run versus the time line line-synchronized 16.6̄ ms intervals for a sampling of PMT-equipped detector channels in E896.

pedestal for all events in a particular 60 Hz time bin (abscissa), for the same sampling of E896 PMTs across different detector systems that were shown in Fig. 3.

In any one of these frames, the average ADC value are the same at the extreme values, indicating continuity and the appropriateness of the present 60 Hz clock-based corrections. It is also interesting to note in Fig. 7 (or Fig. 3) that frequency modes that are some multiple of 60 Hz are also clearly present. An analysis of the frequency spectra obtained from Fourier transforms of these line-shapes for each of the $\sim 380$ PMTs in the E896 TOF system will be presented in the next section.

In all subsequent passes through the experimental data, the value of the ramp ADC in each experimental event is then used to look up $\sim 600$ values from the $\sim 600$ profile histograms recorded in the previous pass. For each detector channel in this event, the appropriate 60 Hz-time-dependent pedestal is subtracted from the detector channel's ADC value, whether or not there is a "hit" in this particular detector channel in this event. The ADC pedestal is then, in software, completely restored to the much tighter distribution expected in the absence of the correlated noise. The resolution for "hits" may also be improved.

Examples of the dramatic improvement to correlated noise problems in these data is shown in Figs. 8 and 9. In either figure, the upper left frame is, for reference, a correlation between a TOF ADC pedestal and a TOF bPMT pedestal. This TOF pedestal is plotted versus the (dual pedestal subtracted) ramp ADC value, i.e. the time in AC line synchronized $16.\overline{6}$ ms intervals, in the lower left frame. The comparison of the two corrections, one based on this bPMT ADC and the other based on the ramp ADC, is shown in the right frame. The raw pedestal is shown as the solid histogram, the pedestal following the bPMT correction is the dotted histogram, while the pedestal following the ramp ADC correction is the dashed histogram.

One observes in the right frame of Fig. 8 that the bPMT correction leads to only a partial correction, while in the right frame of Fig. 9, the bPMT

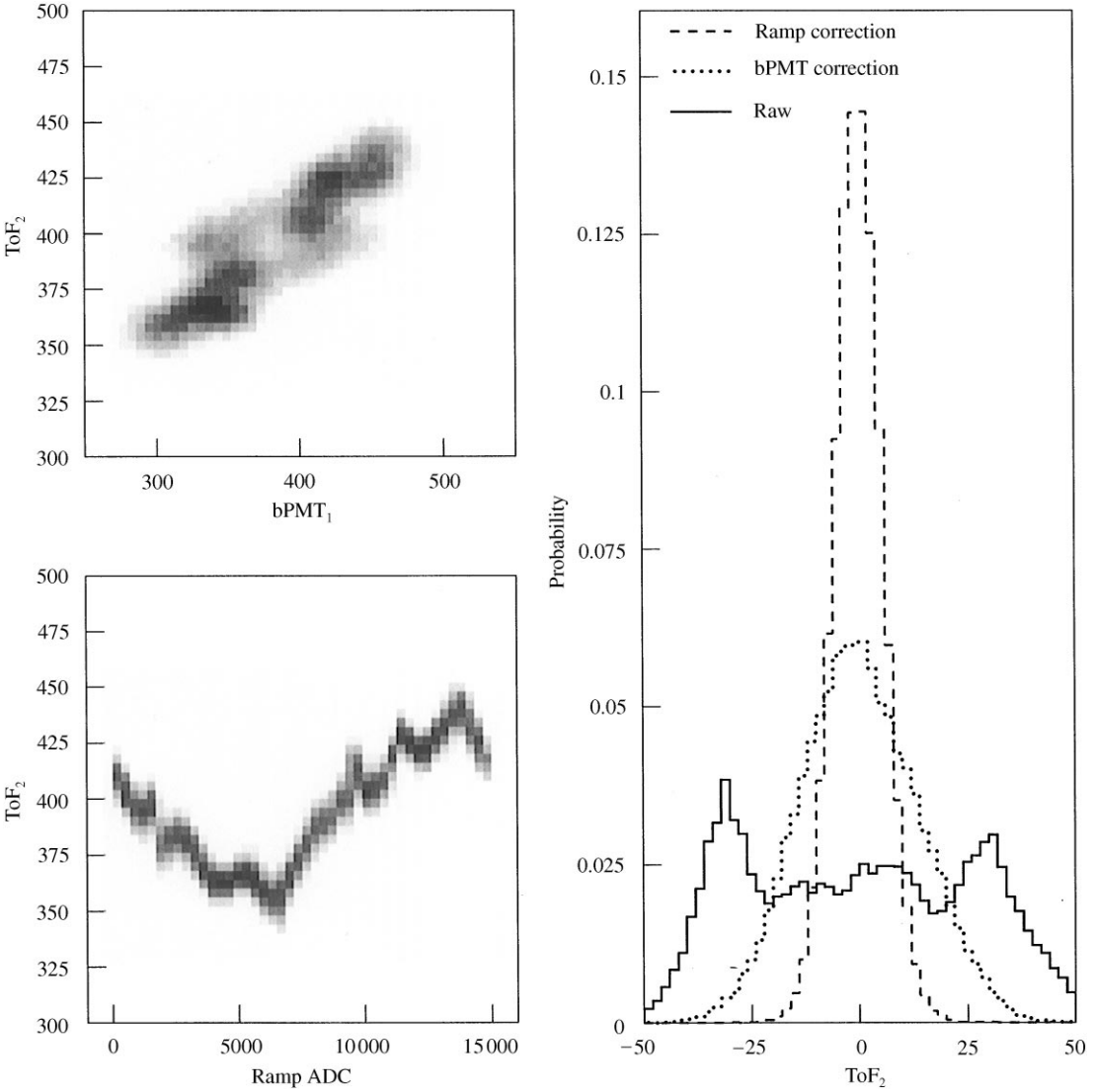


Fig. 8. The comparison of correlated noise corrections based on bPMTs and the present clock circuit for the same two channels (one from the TOF and one a TOF bPMT) shown in the left frame of Fig. 2. The axis out of the page in the left frames is linear.

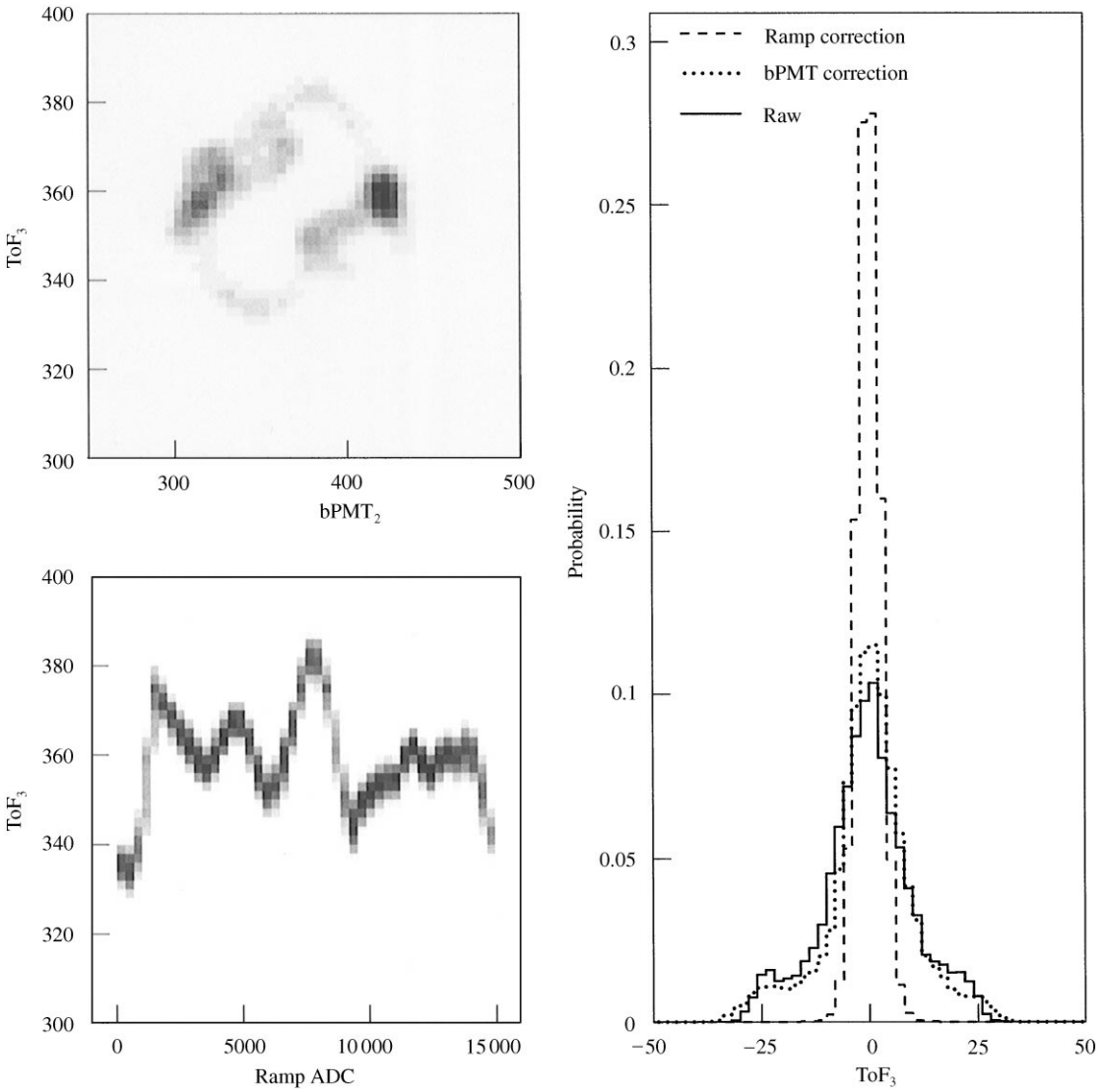


Fig. 9. The same as Fig. 8, but for the same channels shown in the right frame of Fig. 2.

provides no significant correction at all. This is due to the poor correlations seen in the upper left frames. However, as seen in both of the lower left frames, a far stronger correlation exists between the TOF pedestals and the ramp ADC values, allowing an efficient and complete correction. According to the two right frames of these figures, the ramp correction restores the ADC pedestals to perfect Gaussian's with a variance of 3–5 channels – as would be expected in the absence of correlated noise.

## 5. Spectral analysis

That the time dependence of the value of any E896 ADC pedestal is manifestly periodic at 60 Hz is apparent from the tight correlation, and the

continuity at the endpoints, of the profiles shown in Figs. 3 and 7. This makes no statement on higher frequency modes though. As the correlated noise is absent when only the experiment itself is fully powered, but is present during full beam-on running, one suspects a contributor to correlated noise at the AGS is the massive power supplies connected to the numerous beam-line magnets. These regulate at 720 Hz in multiples of 60, so one might expect that frequency modes that are multiples of 60 Hz exist in the line-synchronized time dependence of the ADC pedestals. To investigate this possibility, the measured values of the ADC pedestals versus the time from our 60 Hz clock are Fourier analyzed to extract frequency spectra.

For each of the $\sim 384$ channels of the TOF system, the ADC pedestal versus ramp ADC profile, e.g. Fig. 7, was measured using the data from a single data run. For each profile, an array of dimension $2^{11}$ was filled with 60 copies of this profile placed end to end in this array. This array thus contains an average PMT pedestal as a function of the time in $2^{11}$ bins that spans a total period of 1 s. The Fourier transform of this array then contains the weights for frequencies measured in Hertz.

A typical frequency spectrum is shown in Fig. 10. The weight for the zero frequency mode, which is related to the (time independent) mean value of the pedestal, is suppressed in this histogram. The dominant frequency modes are identified as the bins in this histogram with the largest absolute values of the Fourier coefficient in this bin. The statistical nature of the mean ADC values versus the 60 Hz time used as input to the Fourier transforms results in a finite weight for all possible frequency modes. For the TOF channel shown in this figure, the dominant mode is 60 Hz, although there is significant weight in modes at 300 and 420 Hz.

For each of the 384 channels of the E896 TOF system and in one run, the first and second largest Fourier coefficients were located for each channel using this procedure. The histogram of the number of TOF detector channels having a particular value of the frequency with the largest(second largest) Fourier coefficient is shown in the left(right) frame of Fig. 11. Roughly half of the channels of the E896 TOF system have pedestals that depend on time with the dominant frequency mode being exactly 60 Hz. However, the other half of the TOF channels have ADC pedestals that depend on time dominantly at frequencies that are 3, 5, or 7 times 60 Hz. Even multiples of any significance were not seen in the dominant frequency mode (left frame), although there are channels for which even multiples contribute to the sub-dominant mode (right frame).

It is interesting to note that there is a certain amount of correlation between the dominant frequency mode of the time dependence of the ADC pedestal for a given channel and the location of this channel in the apparatus. In principle this

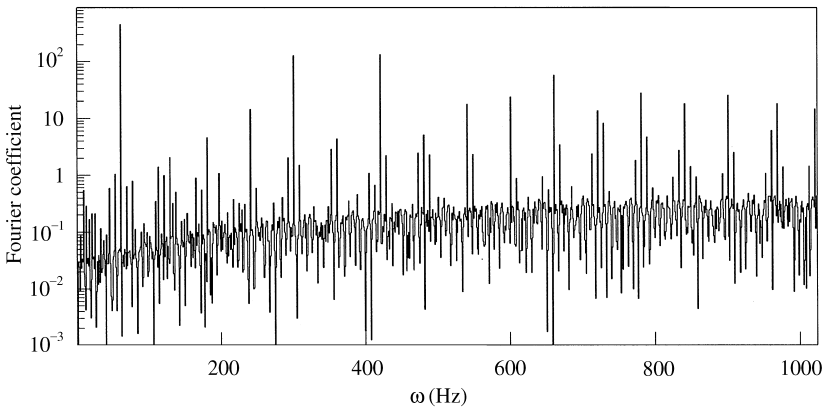


Fig. 10. The Fourier coefficients versus frequency, $\omega$, in Hertz for the correlated noise profile for a particular TOF detector channel.

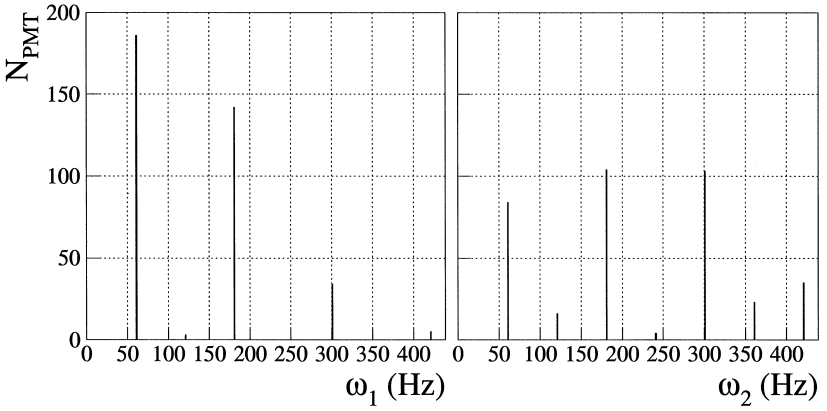


Fig. 11. On the ordinates are histograms of the number of E896 TOF channels that have particular values of the dominant frequency (abscissa, left frame) and sub-dominant frequency (abscissa, right frame).

information could be used to provide more clues as to the exact sources of the correlated noise. In practice, however, this is not necessary, as the off-line 60 Hz clock-based corrections completely solve the problem anyway.

## 6. Summary

A small, highly portable, and inexpensive custom circuit was developed to provide the information needed for an efficient and complete offline correction for correlated noise in all of the $\sim 600$ PMT-equipped detector channels in BNL-AGS Experiment 896. The circuit generates a precision voltage ramp that resets in active synchronization with the AC power, and this ramp voltage is simply digitized in a spare ADC channel to provide line synchronized clock information for every experimental event. The variances of the experimental ADC pedestals following the "ramp ADC" correction were reduced from, in some cases, tens of channels to the values of 3–5 channels expected in the absence of the correlated noise. Experimentally, the correlated noise profiles for each and every PMT was fundamentally periodic and repeating at 60 Hz, yet a considerable number of channels indicate predominant frequencies of odd multiples of 60 Hz, primarily 180 and 300 Hz.

## Acknowledgements

We thank the BNL-AGS E896 Collaboration for the use of preliminary ADC pedestal data from the Au98 run that was discussed above. We gratefully acknowledge funding from the US Department of Energy under Grant No. DE-FG03-96ER40772, as well as helpful comments from H. Takai, S. Costa, C. Nociforo, G.S. Mutchler and E.D. Platner.

## References

[1] http://h0h03.e896.bnl.gov/~bnl896/home_e896.html.
[2] T. Sugitate et al., Nucl. Instr. and Meth. A 249 (1986) 354.
[3] H. Takai, private communication.
[4] S. Costa, private communication.